

## Experimental and Numerical Study of Tidal Basin Management around Link Canal: A Case Study of Bangladesh

Rocky TALCHABHADEL<sup>(1)</sup>, Hajime NAKAGAWA, Kenji KAWAIKE and  
Kazuyuki OTA<sup>(2)</sup>

(1) Department of Civil and Earth Resources Engineering, Kyoto University

(2) Central Research Institute of Electric Power Industry, Japan

### Synopsis

The construction of series of polders is the response to the floods. But the obstructions led to accelerated silt deposition in the rivers. It causes the severe drainage congestion. Dredging is an enormous task which is costly and again the river faces siltation every time. De-poldering and then controlled flooding in a particular flooding plain as the tidal basin, is not a new way of sediment management. Tidal basin acts as sedimentation trap which allows natural tidal flows up and down in the river system. It is basically shifting the sedimentation from the riverbed to selected tidal basin. An attempt has been made to assess the effectiveness of the system through experimental and numerical simulation. It is found that if the natural river is in equilibrium, the recommended size of the link canal is more or less equal to the natural width of the river. Furthermore, if the upstream river flow is reduced, it has resulted in more sedimentation in selected tidal basin.

**Keywords:** Tidal Basin Management, beel, tidal basin, Suspended Sediment Concentration, tidal movement, link canal

### 1. Introduction

For eras, the Bengal delta that constitutes Bangladesh and India's West Bengal has been formed by the sediments carried downstream by *Ganges, Meghna* and *Brahmaputra* river system. In Bengali, Bangladesh is called *nodimatrik desh* (Islam, 2001). This means the rivers gave birth. The Bengal delta has been home to a dynamic interplay of water and land (Staveren *et al.*, 2017). The South West (SW) region of Bangladesh is a tidal basin active tidal channels and large parts are still going through active deltaic formations (Haque *et al.*, 2015). It is characterized by unique brackish water ecosystem interspersed with sensitive tide-dominated rivers, streams and water-filled depressions. A considerable area in the SW region is below the high water level of spring tide.

### 2. Literature review

#### 2.1 Sediment management from impoldering to de-poldering

Before construction of the polders, river tides would inundate vast tracts of lowland twice a day due to astronomical tide from the Bay of Bengal (Rahman and Salehin, 2013; Tutu, 2005). Much of these lowlands are *beels*, a Bengali term used for relatively large depressions that accumulate water (Banglapedia, 2012). The Coastal Embankment Project (CEP) was a response to the large flood in 1954. Construction and development of embankments started in 1961. The polders were constructed into encircled earthen embankments around depressions keeping the main tidal channel outside the polder. The embankments were not constructed to protect against water levels during

cyclones.

The initial outcomes of the polders were quite rewarding both economically and socially. The polder embankments not only prevented floods from overflowing the land but also halted the deposition of silt and clay on the former floodplains. The obstructions by polder system led to accelerated silt deposition and sediment accumulation in region's rivers and channels. The resulting dearth of land formation left floodplains inside the polders lower than riverbanks outside the polders (Rezaie and Naveram, 2013). Vast tracts of land went under water semi-permanently, i.e. for 6 months or more in a year, as the water could not be drained away overland, nor could it be discharged.

To solve this issue, a certain area is kept aside as tidal floodplain by doing temporary de-poldering. The link canal so created connects the tidal basin (selected *beel*) with the river (Ibne Amir et al., 2013). Muddy water enters the tidal basin during high tide with a thick concentration of sediments, depositing a major portion of suspended sediments before flowing back towards the sea during low tide (Ibne Amir et al., 2013; Khadim et al., 2013; Kibria, 2011). Institutionally it was termed Tidal River Management (TRM).

## 2.2 Concept of TRM/TBM

TRM is the scientific term given to the age-old practice of flood and water management where a temporary de-poldering is done by connecting the tidal rivers with designated low land. The concept is simple. The natural high tide of river enters the low lying *beel*, leaves a part of sediment to be deposited and goes back to the ocean. Since this process does not allow sediments to be deposited on the river bed, the depth of river bed also increases and makes the river congestion free (Shampa and Pramanik, 2012). In addition, if the riverbed decline advances, the influence would be exerted to the upper stream. Akai et al. (1990) termed it "The UTSURO". The process is continued for several years (usually 3 to 4 years, the duration depends on the size of the tidal basin). Such tidal basins are to be rotated among various lowlands within the system so that farmers of one tidal basin do not have to suffer for a long time, the process known as Tidal Basin Management (TBM).

TBM involves the natural tide movement in rivers

and taking full advantage of it (Ibne Amir et al., 2013; Shampa and Pramanik, 2012; Talchabhadel et al., 2016a). Fig. 1 shows the conceptual model of TBM. This sedimentation would occur into the riverbed if it is not utilized for storage as sedimentation trap (Ibne Amir et al., 2013; Paul et al., 2013; Rahman and Salehin, 2013).

When one TBM beel has achieved the required raising of the land, then another TBM beel will take the sediment load that comes in with the tide. There should not be any time gap in between closing and operation of successive *beels* (Ullah and Mahmud, 2017). If the rotation is not carried out systematically, then the tides are very likely to drop their sediments in the river channel themselves (Nowreen et al., 2014). Since the TBM process is the participatory approach where the people of identified beel have to sacrifice their land for an intended period (3-5 years), a proper compensation to the affected people should be ensured.

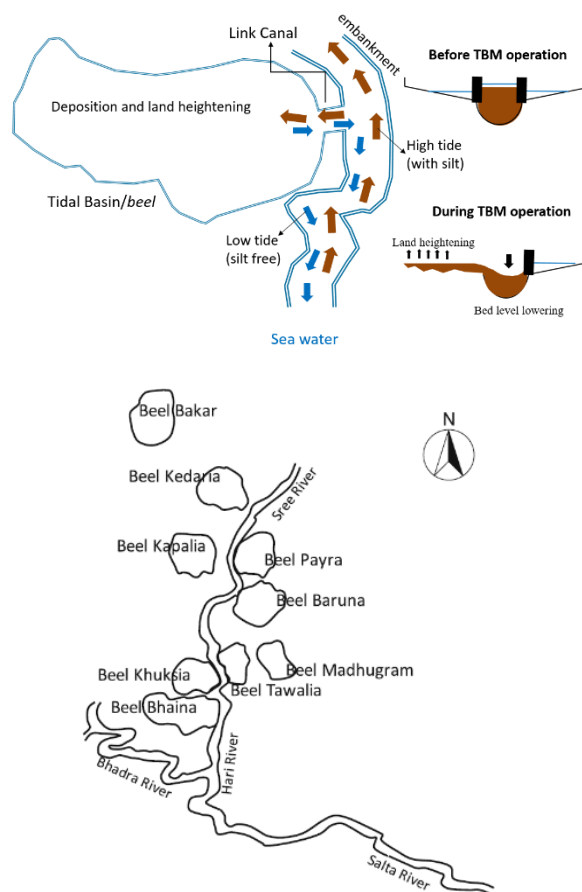


Fig. 1 Conceptual model of TRM/TBM (Source : Author ) and location of proposed tidal basin in KJDRP (Source: Rahman and Salehin, 2013)

### 2.3 Tidal prism – Inlet area relationships

Jarrett (1976) has investigated to develop the tidal prism and inlet area relationship originally developed by O'Brien in 1931 as an empirical relationship based on 10 tidal inlets. The study focused on the determination of the effect of inlet configuration for a number of realistic inlet shapes and tidal conditions. The first known published relationship between the cross-sectional area of the tidal inlet and the tidal prism were given by LeConte in 1905 for harbor entrances on the Pacific coast. The obvious fact that large inlets are found at large bays whereas small inlets at small bays suggested O'Brien (1969) suggested a relationship between equilibrium flow area and tidal prism.

$$A = a * P^n \quad (1)$$

where  $A$  is the minimum flow cross section of the entrance,  $P$  is the tidal prism corresponding to the diurnal or spring range of tide and  $a$  &  $n$  are coefficients vary from entrance to entrance. Stive and Rakhorst (2008) has reviewed some of the popular Dutch and US empirical relationships between inlet cross-section and tidal prism with theoretical elaborations both qualitatively and quantitatively. Many researchers (Hume and Herdendorf, 1993; O'Brien, 1969; Powell *et al.*, 2006; Rakhorst, 2007; Van de Kreeke and Haring, 1980) have suggested to applying the Equation 1 with best-fitting values of  $a$  and  $n$ . The approach of Kraus (1998) is somewhat different. He introduced the representative shear stress needs to attain a value of the magnitude of the critical shear stress for sediment motion.

$$\tau_{*c} \left( \frac{\sigma}{\rho} - 1 \right) g d = g \frac{u^2}{C^2} = g \left( \frac{2P}{CAT} \right)^2 \quad (2)$$

where  $\tau_{*c}$  is critical shear stress according to Shields,  $\sigma$  is the density of sediment particles,  $\rho$  is the water density,  $d$  is the diameter of sediment particles,  $u$  is the characteristic flow velocity (realizing discharge  $Q = A * u$ ,  $Q_{max} = 2P/T$  where  $T$  is the tidal period) and  $C$  is dimensionless Chezy coefficient.

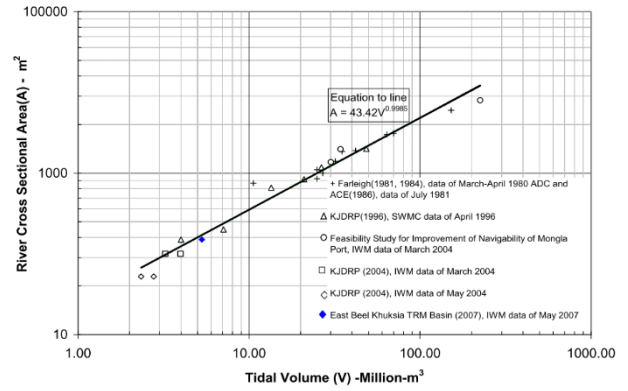


Fig. 2 Equilibrium relationship between tidal prism and river cross-sectional area (Source : Rahman et al., 2015; Shampa and Pramanik, 2012)

Some rearrangement of Equation 1.1 gives

$$A = \left( \frac{4}{\tau_{*c} \left( \frac{\sigma}{\rho} - 1 \right) g d C^2 T^2} \right)^{1/2} P \quad (3)$$

The equation (3) could be compared with equation

$$1.1 \text{ where } a = \left( \frac{4}{\tau_{*c} \left( \frac{\sigma}{\rho} - 1 \right) g d C^2 T^2} \right)^{1/2} \text{ and } n = 1. \text{ Stive}$$

and Rakhorst (2008) has calculated the value of  $a$  to be  $0.9 * 10^{-4}$  for sediment size  $300 \mu m$ . Some researchers have attempted to express the Chezy coefficient in terms of Manning coefficient ( $C = \frac{h^{1/6}}{n}$ ) where  $h$  is characteristics water depth and  $n$  is the Manning coefficient.

From above, it is clear that the entrance cross-section  $A$  and the tidal prism  $P$  could be expressed with a relation. For determining the consistent relationship abundant amount of field-based data of the tidal river is needed because the coefficients vary from entrance to entrance. The sample of one of the equilibrium relationship for a coastal river of Bangladesh is shown in Fig. 2.

### 2.4 Study of TRM/TBM

Many studies have done different types of qualitative analysis of TRM/TBM and its relation with disaster, ecosystem, environment, agriculture, flood, and sediment management. Very limited researchers have attempted to numerically simulate the process of TBM in Bangladesh and almost nil via experimental analysis.

Shampa and Pramanik (2012) has simulated numerically for the *Kobadak* River to assess the effectiveness of proposed TBM in the *beel* Jalalpur. The research proposed that TBM operation is more effective with the construction of the cross dam during the dry period. It is also mentioned that the monsoon flow does not erode the deposited sediment on river bed because of high sediment concentration during monsoon.

Ibne Amir *et al.*, (2013) has numerically simulated in two *beels*: One is East *beel* Khuksia where TBM has fully implemented, and another is *beel* Kapalia where TBM is supposed to operate. The technical feasibilities using economic analysis were analyzed using the numerical modeling. The option that includes, constructing embankments along both banks of the main channels through the tidal basin and thereby allowing sedimentation by gradually cutting the embankment part by part from upstream to downstream, has been suggested in their research. Furthermore, dividing the *beel* into compartment had better results than allowing TBM in the whole basin at the same time. In the research, it is also suggested that the *beels* with greater tidal influence are more suitable for TBM operation.

Rahman *et al.* (2015) has developed a numerical model for two potential *beels*: Sukdebpur *beel* along the left bank of *Betna* River and another *Ticket beel* along the right bank of *Marirchap* River. The research showed that in addition to the dredging/excavation, implementation of TBM to trap up the incoming sediment inside the basin was needed for sustainable sediment and drainage management.

Ogawa and Sawai (2013) has done similar research for the Yellow River for river bed sedimentation control using a tidal reservoir by numerical analysis. In this study, the primary focus is the control of riverbed sedimentation rather than the land heightening or deposition of sediment. Akai *et al.* (1990) called the process of advancement of riverbed decline as “The UTSURO”. The research concluded that the tidal reservoir is effective in a riverbed decline. However, the longer the distance between the connecting point and estuary, the smaller the degree of the river bed decline in the downstream.

### 3. Objectives of the study

The literature review reveals that a number of comprehensive studies on TRM/TBM are available. These studies cover a wide range of analysis regarding appropriate planning, design, and implementation of TBM in a coastal river. Furthermore, such an innovative scientific approach which is again semi-natural process has been related to institutional management, socio-economical barriers by many researchers. The implications of TBM as disaster management approach, ecosystem and environmentally friendly approach and ultimately sustainable sediment management approach have been discussed by them.

Some of the researchers have discussed regarding the mainstreaming of TBM for participatory environmental governance, flood policy, climate change adaptation, disaster management, drainage rehabilitation project and many others. Few researchers also carried out numerical simulation for effective planning, the design of potential *beels* and also for monitoring and evaluation of operated *beels*. It clearly shows the TBM process has been one of the integral parts of sediment management for tidal rivers in Bangladesh. But the experimental analysis of such complicated process is very rare.

In this research, the attempts have been made to assess the effectiveness of TRM/TBM through small-scale laboratory experiments. One significant hydraulic fact is that the faster the flow is, the more sediment it can carry with it. One of the key governing factors of the flow is the opening size of link canal. For the establishment of a consistent relationship between tidal prism and minimum cross-sectional area, an abundant amount of real field data of the tidal rivers are needed.

To inspect the effectiveness of TBM exploring different opening sizes and to compare with available empirical relations, this research has attempted to carry out small-scale laboratory experiments. Two-dimensional (2D) numerical simulation models have been developed to compare with experimental results and to analyze different alternatives to suggest the sustainable sediment management. The experimental and numerical analysis are implemented to analyze the physical mechanism of the sediment transport and deposition

during the operation of TBM process. The complex phenomena and local mechanism during the experiment around a sharp bend or any structure have attempted to discuss with the real scenario and attempted to analyze by three-dimensional (3D) numerical simulation.

## 4. Experiments and Numerical Simulations

### 4.1 Experimental analysis

The experiments were carried out in a flume located at the Ujigawa open laboratory of Disaster Prevention Research Institute, Kyoto University. The schematic view is illustrated in Fig. 3. See (Talchabhadel et al., 2017a, 2017b) for a detailed explanation of the experimental methodologies. TBM capitalizes on the natural movement of tidal water. To represent alternative high and low tidal flow, an adjustable gate was used. To represent high tide, the gate was closed for 2 mins and downstream flow from water pump was supplied along with dry sediment supply from sediment feeder. After then, the gate was opened for next 2 min. At that time downstream supply of water and sediment were stopped representing low tide. Same processes were repeated. Two complete tidal cycles in a day in the real case of Bangladesh (Kibria, 2011) here is attempted to represent with 8 min experimental case (i.e. 2 min high tide and 2 min low tide for one tidal cycle). Four cases with different opening sizes were investigated varying the size of the opening canal towards tidal basin.

### 4.2 Numerical Simulations

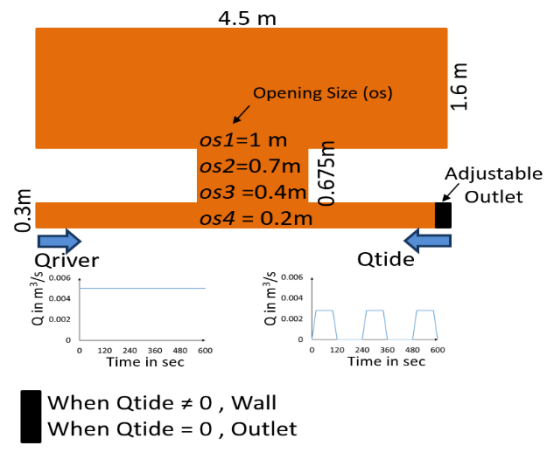


Fig. 4 Boundary condition treatment in numerical simulation

The experimental boundary condition of an adjustable condition has been applied in the numerical simulation (shown in Fig. 4). The boundary at outlet shown in black in Fig. 4 switches to the side wall and the outlet along with the time. When the boundary at outlet switches to the side wall, the input high tidal discharge and sediment supply are also provided.

#### 4.2.1 2D simulation

The simulation model used in this study is structural gridded two-dimensional (2D) unsteady flow model based on a shallow-water equation. Finite Difference Method (FDM) is applied. To solve the equations, leap frog difference scheme is employed.

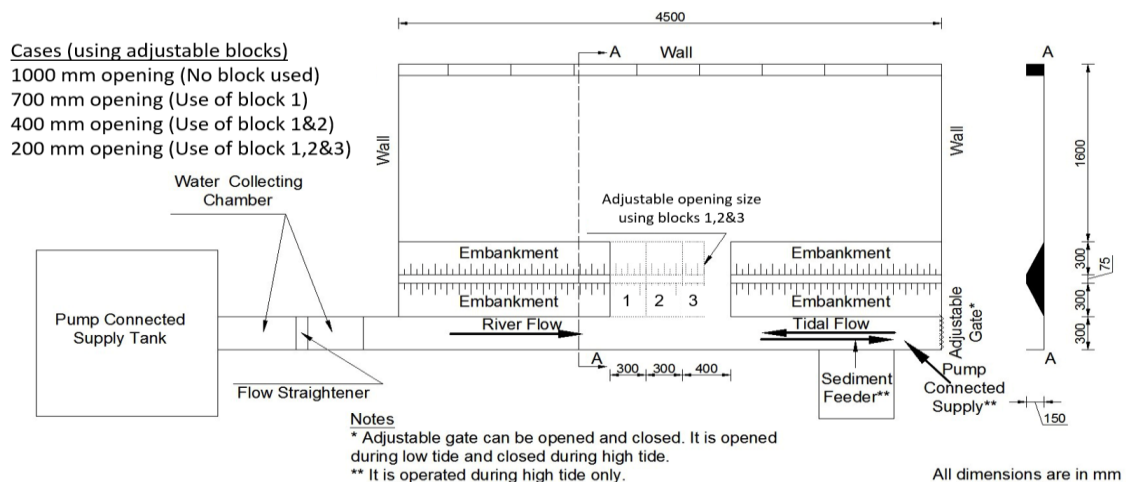


Fig. 3 Schematic view of experimental setup

### Continuity equation

$$\frac{\partial h}{\partial t} + \frac{\partial M}{\partial x} + \frac{\partial N}{\partial y} = 0 \quad (4)$$

### Momentum equation

$$\frac{\partial M}{\partial t} + \frac{\partial(uM)}{\partial x} + \frac{\partial(vM)}{\partial y} = -gh \frac{\partial H}{\partial x} - \frac{gn^2 u \sqrt{u^2 + v^2}}{h^{1/3}} \quad (5)$$

$$\frac{\partial N}{\partial t} + \frac{\partial(uN)}{\partial x} + \frac{\partial(vN)}{\partial y} = -gh \frac{\partial H}{\partial y} - \frac{gn^2 v \sqrt{u^2 + v^2}}{h^{1/3}} \quad (6)$$

where,  $h$  is the water depth,  $M (=uh)$  and  $N (=vh)$  are fluxes in the  $x$  and  $y$  directions,  $u$  and  $v$  are velocities in the  $x$  and  $y$  directions,  $H$  is the water level,  $g$  is the acceleration of gravity, and  $n$  is the Manning's roughness coefficient. Sediment transport is simulated using the following equations:

### Suspended sediment transport calculation

Suspended sediment transport is simulated using the following equations.

$$\frac{\partial(C_h)}{\partial t} + \frac{\partial(CM)}{\partial x} + \frac{\partial(CN)}{\partial y} = D \left( \frac{\partial^2(C_h)}{\partial x^2} + \frac{\partial^2(C_h)}{\partial y^2} \right) + E + Cw \quad (7)$$

where  $C$  is the concentration of sediment,  $D$  is a coefficient of diffusion,  $E$  is the parameter of flowing up and  $w$  is the settling velocity. Given the situation,  $D$  was set to  $0.1 \text{ m}^2/\text{s}$  (Hashimoto *et al.*, 2016).

In this study, the settling velocity is calculated with the Rubey's formula (Rubey, 1933).

$$w = \sqrt{\frac{2}{3} \left( \frac{\sigma}{\rho} - 1 \right) gd} + \frac{36v^2}{d^2} - \frac{6v}{d} \quad (8)$$

where  $\sigma$  is the density of sediment particles,  $\rho$  is the water density,  $d$  is the diameter of sediment particles and  $v$  is the coefficient of kinematic viscosity of water.

The upward flux is assumed to be under equilibrium condition. The equilibrium concentration is calculated using the van Rijn empirical formula (Van Rijn, 1984a).

$$E = wC^* \quad (9)$$

$$C^* = 0.015 \frac{dT^{1.5}}{aD_*^{0.3}} \quad (10)$$

where  $a$  is the reference is level taken  $0.05h$ ,  $D_*$  is the particle size parameter and  $T$  is a dimensionless excess bed shear stress parameter.  $D_*$  and  $T$  are defined by the equation 3.8 and 3.9.

$$D_* = d \left[ \frac{(\frac{\sigma}{\rho} - 1)g}{v^2} \right]^{1/3} \quad (11)$$

$$T = \frac{\tau_* - \tau_{*c}}{\tau_{*c}} \quad (12)$$

where  $\tau_*$  and  $\tau_{*c}$  are the dimensionless shear stress and critical shear stress according to the Shields. The grain related shear stress parameter  $\tau_*$  is calculated by considering Chezy's equation.

$$\tau_* = \frac{u_*^2}{\left( \frac{\sigma}{\rho} - 1 \right)gd} \quad (13)$$

$$u_* = \sqrt{g} \frac{u}{C'} \quad (14)$$

where  $C' =$  grain related Chezy's roughness coefficient which for rough flow is given by :

$$C' = 18 \log \left( \frac{12h}{k_s} \right) \quad (15)$$

where  $k_s =$  grain roughness. For smooth bed,  $k_s = 0$ , and for a stationary flat bed in laboratory experiments,  $k_s$  is usually set to the median diameter  $d_{50}$  of bed material because there is only sand-grain roughness on the bed. For stationary flat bed in real rivers,  $k_s$  should theoretically also be about  $d_{50}$ , but in practice usually somewhat higher values are adopted, e.g. Van Rijn (1984b) relate the grain roughness to the coarse 90<sup>th</sup> percentile ( $d_{90}$ ) of grain size distribution, i.e.  $k_s = 3d_{90}$ . By contrast Engelund and Fredsøe (1976), Nielsen (1992) and Soulsby and Damgaard (2005) related the grain roughness to the median grain size ( $d_{50}$ ) i.e.  $k_s = 2.5d_{50}$  which is used in the present study. The dimensionless critical shear stress  $\tau_{*c}$  for the sediment size  $d$  is evaluated with the Iwagaki formula (Iwagaki, 1956).

$$\tau_{*c} = \begin{cases} 0.05 & \text{if } R_* \geq 671.0 \\ 0.00849R_*^{3/11} & \text{if } 162.7 \leq R_* < 671.0 \\ 0.034 & \text{if } 54.2 \leq R_* < 162.7 \\ 0.195R_*^{-7/16} & \text{if } 2.14 \leq R_* < 54.2 \\ 0.14 & \text{if } R_* < 2.14 \end{cases} \quad (16)$$

where

$$R_* = \frac{\sqrt{(\frac{\sigma}{\rho}-1)gd^3}}{\nu} \quad (17)$$

### Bedload transport calculation

The bed load transport rate is calculated by the equation of (Ashida and Michiue, 1972).

$$\frac{q_b}{\sqrt{(\frac{\sigma}{\rho}-1)gd^3}} = 17\tau_{*e}^{\frac{3}{2}} \left(1 - \frac{u_{*c}}{u_*}\right) \left(1 - \frac{\tau_{*c}}{\tau_*}\right) \quad (18)$$

where  $q_b$  is the bed load discharge ( $m^2/s$ ),  $\tau_*$ ,  $\tau_{*c}$  and  $\tau_{*e}$  are dimensionless shear stress, critical shear stress (Iwagaki, 1956) and effective shear stress, respectively;  $u_*$  and  $u_{*c}$  are friction velocity and critical friction velocity ( $m/s$ ), respectively. These parameters are calculated through following relations:

$$\tau_{*c} = \frac{u_{*c}^2}{(\frac{\sigma}{\rho}-1)gd} \quad (19)$$

$$\tau_{*e} = \frac{u_{*e}^2}{(\frac{\sigma}{\rho}-1)gd} \quad (20)$$

where  $u_{*e}$  is effective friction velocity. The effective shear stress  $\tau_{*e}$  is calculated by taking the account of equivalent roughness height  $k_s$  quantifying the influence of roughness elements such as sand grains, sand waves (including ripples, dunes and antidunes) and other bed form. For sand wave bed,  $k_s$  should be related to the height of the sand waves, (Van Rijn, 1984b) proposed the following relationship, which is used in the present study to replicate the bed form of experimental result.

$$k_s = 2.5d_{50} + 1.1\Delta(1 - e^{-25\psi})(25 - T) \quad (21)$$

where  $T$  is an excess bed shear stress parameter defined earlier and  $\psi = \frac{\Delta}{\Lambda}$ , is the bed-form steepness,  $\Delta$  and  $\Lambda$  the height and length of the bed forms. The bed-form steepness is calculated from

$$\psi = \frac{\Delta}{\Lambda} = 0.015 \left(\frac{d_{50}}{h}\right) (1 - e^{-0.5T})(25 - T) \quad (22)$$

### Bedload deformation

The bed level changes are computed from the information of bed load and suspended load transport rates using the mass-balance equation.

$$(1 - \lambda) \frac{\partial z_b}{\partial t} + \frac{\partial q_{bx}}{\partial x} + \frac{\partial q_{by}}{\partial y} + (E - Cw) = 0 \quad (23)$$

where  $\lambda$  is the sediment porosity,  $q_{bx}$  and  $q_{by}$  are bed load transport rates in the x and y directions.

### 4.2.2 3D simulation

The simulation model used in this study is OpenFOAM (Open Field Operation and Manipulation which is primarily a C++ toolbox for the customization and extension of numerical solvers for continuum mechanics problems, including computational fluid dynamics (CFD). It comes with a growing collection of pre-written solvers applicable to a wide range of problems. It is released open source under the GPL (OpenCFD Ltd., 2009a, 2009b).

The hydrodynamic model consists of a RANS (Reynolds-averaged Navier-Stokes) model,  $k-\omega$  SST (shear stress transport) turbulence closure, and a volume of fluid (VOF) method for capturing the water surface (Ota *et al.*, 2016). The computational domain is represented by a collocated mesh of triangular prismatic cells (shown in Fig. 5) that fits on the bed topography. The computational domain consist of three boundaries: inlet, outlet and walls (i.e. the bed and the surface of hydraulics structure). At the inlet boundary, the water depth is automatically determined from the VOF computation by specifying inflow rate. The cross-sectional average velocity is evenly set to the inlet velocity.

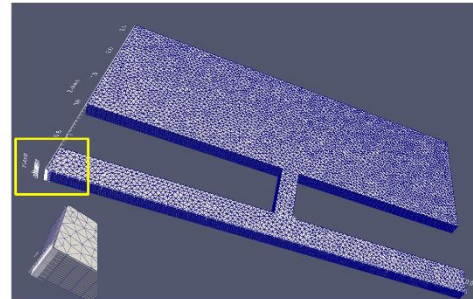


Fig. 5 Computational meshes for 3D model (unstructured 2D with vertically structured)

The transverse and vertical velocity components are specified as zero. Turbulence quantities, turbulent kinetic energy  $k$  and specific turbulence dissipation  $\omega$ , are specified as typical values obtained from turbulence characteristics in open-channel flow shown by Nezu and Nakagawa (1993). At the outlet boundary, zero-gradient conditions, the Neumann conditions are applied for all quantities. At the wall boundaries, zero velocity is specified for the three components of the velocity. Turbulent kinetic energy  $k$  is specified for Neumann condition. The specific turbulence dissipation  $\omega$  is specified for a blending function on dimensionless wall distance suggested by Menter *et al.* (2003).

The governing equations are the 3D continuity and RANS equations for incompressible flows and the advection equation of the  $F$ -function used in the VOF method, which can be written in the vector form as

$$\nabla \cdot \mathbf{U} = 0 \quad (24)$$

$$\frac{\partial \rho \mathbf{U}}{\partial t} + \nabla \cdot (\rho \mathbf{U} \mathbf{U}) = -\nabla p + \nabla \cdot \boldsymbol{\tau} + \rho \mathbf{g} + \mathbf{f}_s \quad (25)$$

$$\frac{\partial F}{\partial t} + \nabla \cdot (\mathbf{U} F) = 0 \quad (26)$$

where  $\nabla$  = the three-dimensional gradient operator,  $\mathbf{U}$  = the flow velocity vector,  $\rho$  = the fluid density,  $p$  = the pressure,  $\boldsymbol{\tau}$  = the viscous stress tensor,  $\mathbf{g}$  = the gravitational acceleration vector, and  $\mathbf{f}_s$  = the body force equivalent to the surface tension. The step function  $F$  used in the VOF method is defined to be one at cells occupied by water and zero at cells occupied by air. Cells with  $F$ -function between zero and one contain water surface. In order to solve the velocity-pressure coupling, the PISO (pressure implicit with splitting of operator) approach is adopted. The finite volume method (FVM) is used for discretization, the second-order central difference method for spatial discretization and the first-order implicit method for temporal discretization.

The  $k$ - $\omega$  SST model (Menter *et al.*, 2003), which is often applied to boundary layer flow under inverse pressure gradient, is used to model the closure turbulence. The  $k$ - and  $\omega$ - equations of the  $k$ - $\omega$  SST models are, respectively

$$\frac{\partial \rho k}{\partial t} + \nabla \cdot (\rho \mathbf{U} k) = \nabla \cdot [\rho (v + \sigma_k v_t) \nabla k] + P_k - \beta^* \rho \omega k \quad (27)$$

$$\frac{\partial \rho \omega}{\partial t} + \nabla \cdot (\rho \mathbf{U} \omega) = \nabla \cdot [\rho (v + \sigma_\omega v_t) \nabla \omega] + \frac{C_1}{v_t} P_k - C_2 \rho \omega^2 + 2\rho(1 - F_1) \frac{\sigma_\omega}{\omega} \nabla k \cdot \nabla \omega \quad (28)$$

where  $k$  = the turbulence kinetic energy,  $\omega$  = the specific dissipation of turbulence kinetic energy,  $P_k$  = the rate of turbulence production. The quantities  $\sigma_k$ ,  $\beta^*$ ,  $\sigma_\omega$ ,  $C_1$ , and  $C_2$  are the model coefficients, and  $F_1$  is the so-called blending function. See Menter *et al.* (2003) for details of the model and used coefficients.

The volume of sediment pickup per unit time from a numerical mesh on the bed surface,  $V_p$ , is given by:

$$V_p = \frac{A_3 d}{A_2} p_s S_b \quad (29)$$

where  $A_2$  ( $= \pi/4$ ) and  $A_3$  ( $= \pi/6$ ) = the two- and three-dimensional shape coefficients of the sand grain, respectively,  $p_s$  = the pickup rate, and  $S_b$  = the area of the bed-surface mesh. The pickup rate  $p_s$  is obtained from the empirical equation mentioned above in equation (9) and (10) using Van Rijn (1984a).

This work uses a standard advection-diffusion equation for the Eulerian model of suspended load.

$$\frac{\partial C_s}{\partial t} + \nabla \cdot \mathbf{q}_s = \nabla \cdot \left( \frac{v_t}{\sigma_c} \nabla C_s \right) \quad (30)$$

$$\mathbf{q}_s = \left( \mathbf{U} - w \frac{\mathbf{g}}{|\mathbf{g}|} \right) C_s \quad (31)$$

where  $C_s$  = sediment concentration,  $\mathbf{q}_s$  = flux of suspended sediment,  $v_t$  = turbulence eddy viscosity,  $\sigma_c$  ( $= 1.0$ ) = Schmidt number,  $w$  = sediment settling velocity. The value of  $w$  in clear water is calculated using the relation proposed by Wu and Wang (2006). The effect of sediment concentration on the settling velocity is taken into account using the Richardson and Zaki (1954) relation. The source term and sink term are added to the advection-diffusion equation at bed boundary considering sediment exchange

between bed load and suspended load as:

$$\mathbf{q}_s \cdot \mathbf{n} = \frac{\sum_n V_t^{(n)} - V_{settle}}{S_b} \quad (32)$$

$$V_{settle} = w_s C_s S_b \quad (33)$$

where the summation of  $V_t^{(n)}$  represents the total volume of sediments which is transited into suspension at each time step after pick-up. The existing formula of suspended sediment concentration usually assumes equilibrium state of sediment concentration near the bed and defines the reference height such as 5 % of the water depth used by Van Rijn (1984a). The advection-diffusion of suspended load is therefore solved in whole computational cells in which water occupies:

Using the volumes of sediment pickup and sediment deposition, which are calculated as previously described, the temporal variation in bed elevation is expressed as follows:

$$\frac{\partial z_b}{\partial t} = \frac{A_1 A_2 \sum_n V_d^{(n)} - V_p}{A_3 S_{b,p}} \quad (34)$$

where  $z_b$  = the bed elevation,  $A_1$  (= 1.0) = the shape coefficient of the sediment particles, and  $S_{b,p}$  = mesh area of the bed surface cell projected onto a horizontal plane where sediment is deposited. The summation of  $V_d^{(n)}$  represents the total volume of deposited sediments at each time step after pick-up.

## 5. Results and discussions

The experimental results, verification of the developed numerical models and numerical analysis results are discussed in this section.

### 5.1 Experimental results and discussions

Fig. 6 shows the typical temporal Suspended Sediment Concentration (SSC) variation at the different sampling points [1 - 30] for Case II for 8 min experimental time. Similarly, in all 4 cases, SSCs during the high tides are quite higher than during the low tides. The supplied sediment is transported from the downstream during the high tides, which is mostly deposited in the side basin before coming back during low tides. The realistic

TBM operation has been done in simplistic design with the straight channel of the tidal river and the perpendicular attachment of the side basin via link canal. Blue color here represents the proximity closer to the tidal source whereas green represent the later. Similarly, the gradient color from darker to the lighter represents the distance from the link canal towards the side basin from the cut is increasing.

More the distance from the tidal source, the SSC decreased. The preliminary experimental result carried out by (Talchabhadel *et al.*, 2016b, 2016c) shows that the SSCs towards the flow direction are higher. The detailed investigation of the spatial distribution of SSC is done in subsequent sections. During the low tides, SSC values are very inferior which represents the significant amount of sediment has been trapped in the side basin. Fig. 7 shows the average value of the SSC of the sampling points located at  $0.25*os$ ,  $0.5*os$  and  $0.75*os$  from the end of the link canal towards the tidal source (shown in Fig. 6) where  $os$  is an opening size of the link canal.

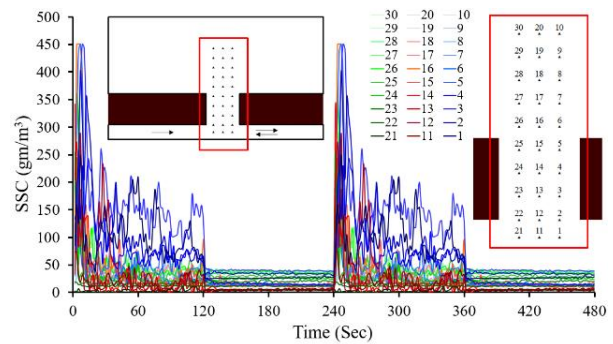


Fig. 6 Typical SSC variation at different sampling points (Case II)

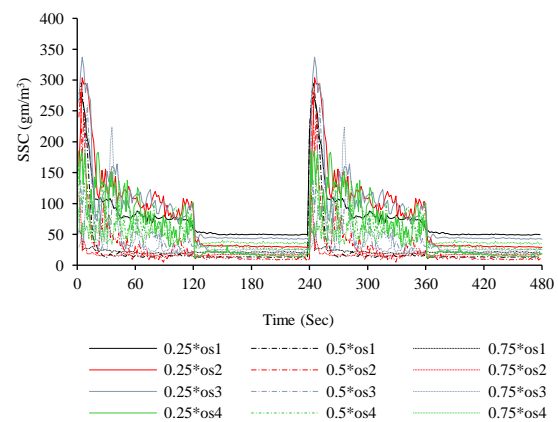


Fig. 7 Typical SSC variation at different sampling points (Case II)

During the high tide, in case I and case II the average values of the SSC at  $0.75*os$  are found to be almost negligible compared to the average values of the SSC at  $0.25*os$  i.e. 13.5 % for case I and 15.6% for case II. Again, the average values of the SSC at  $0.5*os$  are found to be around one-third of the SSC at  $0.25*os$  i.e. 29.4 % for case I and 36.1% for case II. It clearly indicated that the larger size of opening has not been utilized for the transport of the sediment. In the case of narrower opening, the opening sizes have been utilized effectively. The average values of the SSC at  $0.75*os$  are found to be around half of the SSC at  $0.25*os$  i.e. 46.37 % for case III and 57.7 % for case IV. Again, the average values of the SSC at  $0.5*os$  are found to be significant with more than half of the SSC at  $0.25*os$  i.e. 57.3 % for case III and 78.9 % for case IV.

During the low tide, the SSC measured at sampling points around the link canal shows greater values in the narrower opening cases (i.e. case III and case IV) than the wider opening cases (case I and case II). It indicates that during the low tide, the water coming back from the side basin has greater shear stress in narrower opening cases than wider opening cases which promotes in the erosion of deposited sediment around the link canal which effectively demonstrates the phenomena of TBM. Fig. 8 shows the typical spatial distribution of SSC for Case IV for 4 min experimental time. The line graph at the top shows the temporal variation of the SSC at the black dotted location shown in Fig. 8.

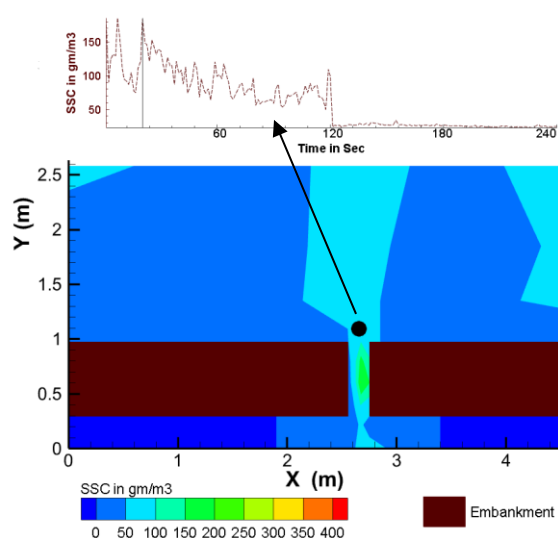


Fig. 8 Typical SSC spatio-temporal variation (Case IV)

Compared to the SSCs at high tide, the SSCs at low tide are almost constant throughout and the magnitude of SSCs are also very lesser compared to SSCs at high tide. In space, the lateral distribution of SSC is more or less symmetrical progressing from the opening of the link canal. It also shows similar results of the greater the distance from the tidal source, lesser is the SSC. But due to the limited size of the side basin, the wall effects are clearly seen. The SSCs at the sampling points near to the side walls are higher than the nearby sampling points.

The bed level measurements from the laser displacement sensor were done around the link canal. Fig. 9 shows the final bed level condition after 10 hours of the experiment for all 4 cases. In case I, it is quite clear that the spacious width has not been properly consumed for the sediment transport and deposition. In case II, the sediment has been transported and deposited in a substantial amount but on the link canal itself, a huge amount of sediment gets deposited. The flow during the low tide, when it flows out from the side basin, has not sufficient shear stress to erode the deposited sediment around the link canal. In case III, a significant amount of the sediment has been transported and deposited in the side basin along with significant erosion during the low tide. Similarly, in case IV, the shear stress developed during the low tide is sufficient to erode the sediment from the link canal.

The latter two cases (i.e. case III and case IV) that are nearly equaled to the width of the river effectively demonstrates the realistic operation of TBM which is needed to solve the drainage congestion. To suggest the optimum size of the opening size, more experiments supported by numerical simulations are needed with varying opening sizes. Further analysis has been done subsequent section using the numerical simulation to represent the experimental condition. The current experimental research has demonstrated effective TBM process in the narrower opening cases (case III and case IV) rather than wider opening sizes (case I and case II). Moreover, it can also be inferred that if the existing river is not constrained by any civil structure and human interventions (i.e. it is in tidal equilibrium), then the recommended opening size of the link canal is almost equaled to the natural width of the river.

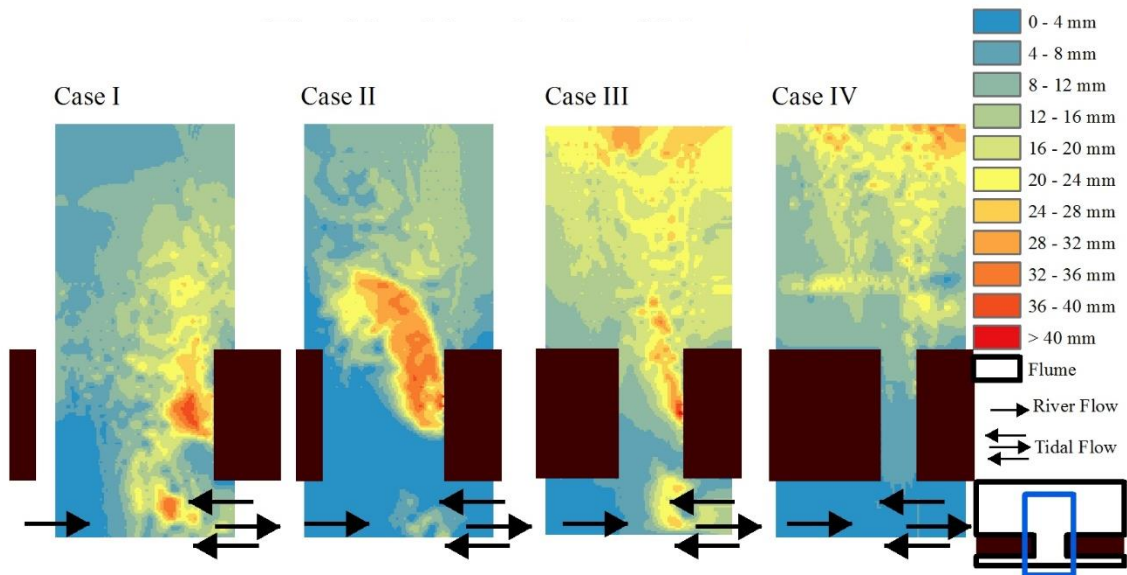


Fig. 9 Final bed level after 10 hours (all 4 cases)

For the measurement of spatially large area and when due to different experimental circumstances, it is difficult to measure with a sophisticated instrument like laser displacement sensor throughout the area of interest, the alternative way to measure spatial bed level elevation can be done by the photogrammetric processing. The digital images with 5568 X 3712 [pixel size (mm) = 0.00239464 X 0.00239464] and focal length (10 mm) were taken from different angles and different heights shown in Fig. 10 (top). 164 images were processed photogrammetrically to generate three-dimensional spatial data. 76965 points, 9827695 dense cloud, and 295506 faces were generated to produce 3D topography. Generated 3D topographical data was geo-referenced at known control points as shown in Fig. 10 (bottom).

The accuracy of the photogrammetrically analyzed bed level is checked with the laser displacement sensor at 2711 points and they both have an acceptable agreement with 2.45 percent bias, 0.4 mm mean error and coefficient of determination 0.82. Fig. 11 shows the bed level extracted by photogrammetric analysis superimposed by the 2711 points measured by the laser displacement sensor. In the case of experiment, the mean error is less than 1 mm which is satisfactory. The 3D spatial data is helpful for the numerical simulation and also helpful for the validation. With the agreeable accuracy, this technique can easily be applied.

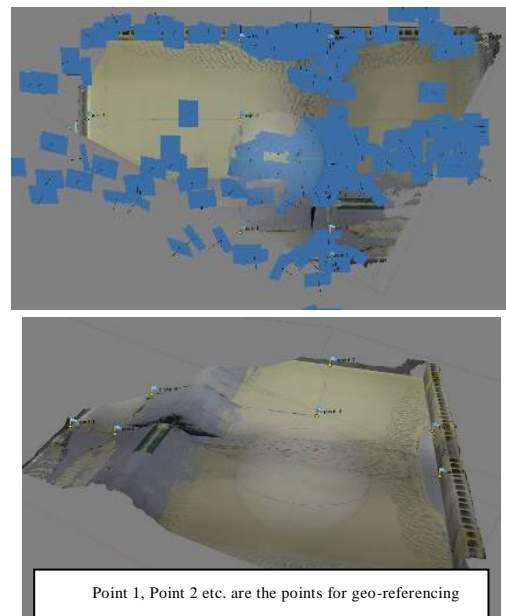


Fig. 10 Photogrammetric analysis for bed level measurement (case IV)

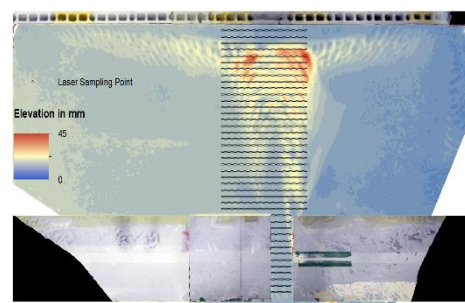


Fig. 11 typical photogrammetric analyzed final bed level after 10 hours superimposed by points measured by laser displacement sensor (case IV)

## 5.2 Numerical model verification

The flow model of 2D and 3D model were firstly verified with experimentally measured water depth and depth-averaged velocity. The sample comparisons of the water depth and flow velocities for one tidal cycle (i.e. high tide and low tide representation) with measured experimental data for one case are shown in Fig. 12. The water depth has well captured by the simulation model. The rapid temporal fluctuations of velocities with sharp instantaneous variation could not be captured precisely in the numerical simulation. Overall, the model has replicated the experimental condition with good agreements.

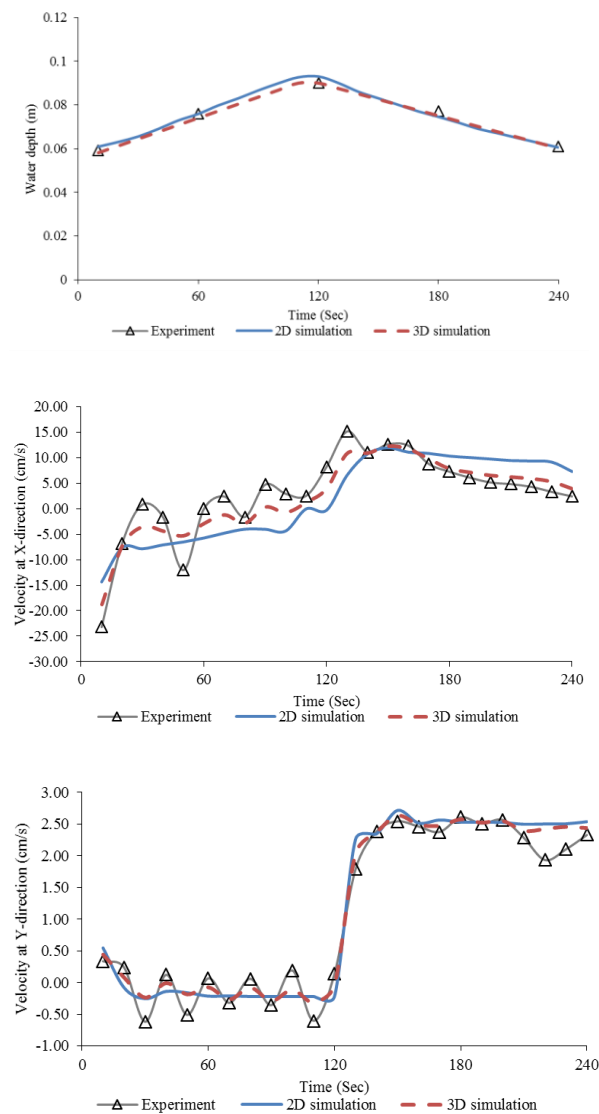


Fig. 12 Sample comparison of simulated and experimental water-depth, x-velocity and y-velocity at midpoint of the link canal (case IV)

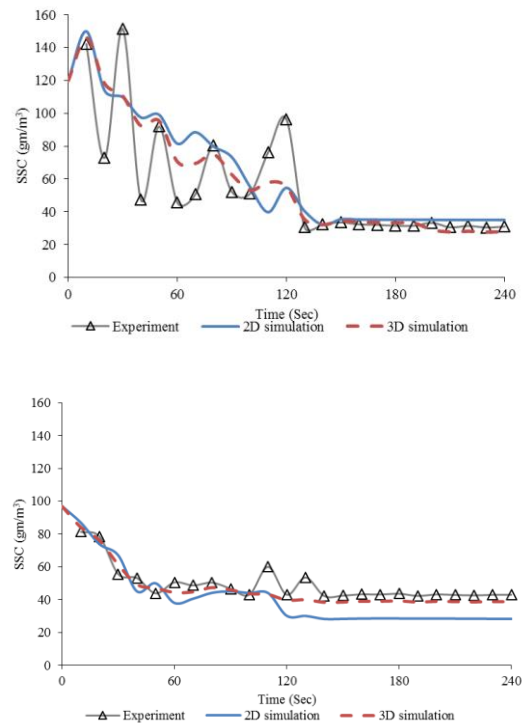


Fig. 13 Sample comparison of simulated and experimental SSC around link canal [top] and around tidal basin [bottom] (case IV)

The sample comparisons of the SSCs with measured experimental data is shown in Fig. 13. One of the reasons behind the sharp fluctuations of SSCs resulted from sharp instantaneous variation of velocities might be the input supply of the discharge from the pump from the downstream as tidal source. Moreover, the dry sediment supply during the experiment is not uniform throughout. The drop of the larger portion of sediment at once happens several time resulting higher SSC at that moment compared to other time. Overall, the quantity and volume of the sediment has been well represented by developed numerical models.

The temporal changes of the bed level have not been measured via experiment, only the final bed level condition was measured in the experiment. The final bed level has been measured by using laser displacement sensor and photogrammetric analysis. The validity of the numerical model is checked for the final bed level condition. The sample comparison of the bed level after 10 hours of repetitive high and low tides is shown in Fig. 14. The spatial distribution of deposited sediment has shown agreeable congruity with experimental condition.

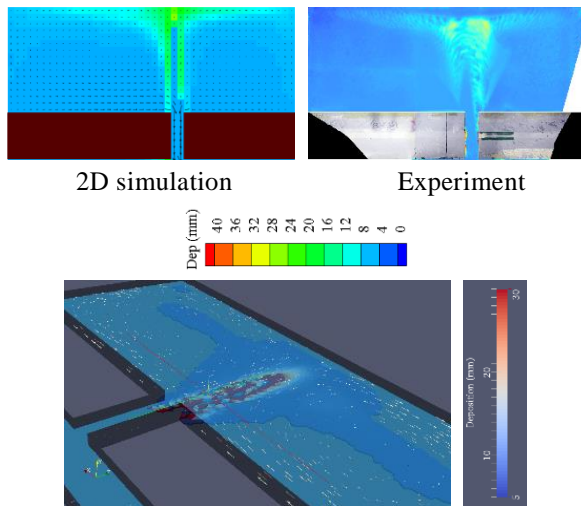


Fig. 14 Sample comparison of simulated and experimental bed level (case IV)

Table 1 Statistical comparison of experimental and simulated results

Percent Bias					
SN	Description	Parameters			
		Water depth	Velocity (magnitude)	SSC	Deposition
2D Model					
1	Case I	1.36	2.16	-8.52	1.08
2	Case II	-0.35	0.95	-7.53	3.94
3	Case III	0.81	1.33	-9.18	-0.51
4	Case IV	-1.06	-2.69	-6.28	-1.39
3D Model					
1	Case I	0.83	-1.26	-6.81	0.64
2	Case II	-0.33	-0.28	-5.64	4.89
3	Case III	0.29	1.82	-4.86	1.32
4	Case IV	1.04	-1.56	-5.77	1.16

Coefficient of Determination					
SN	Description	Parameters			
		Water depth	Velocity (magnitude)	SSC	Deposition
2D Model					
1	Case I	0.93	0.84	0.71	0.74
2	Case II	0.98	0.81	0.83	0.79
3	Case III	0.94	0.86	0.74	0.71
4	Case IV	0.91	0.79	0.69	0.82
3D Model					
1	Case I	0.98	0.86	0.81	0.79
2	Case II	0.96	0.91	0.78	0.84
3	Case III	0.97	0.84	0.75	0.73
4	Case IV	0.97	0.87	0.82	0.79

The comparison of the flow velocity, SSC and sediment deposition for all four cases has been tabulated in Table 1. The table illustrates statistical check using Percent Bias (to measure average tendency of the simulated data to be larger or smaller than their observed data) and Coefficient of Determination (to describe the degree of collinearity between simulated and measured data) of the parameters (water depth, magnitude of the velocity, SSC and deposition height) for all four cases with agreeable indication.

### 5.3 Numerical results and discussions

The detailed analysis from the numerical simulation is focused on the deposition of the sediment for following different scenarios.

- Different upstream river flow condition
- Different opening sizes of the link canal

The average value of the deposited sediment after 10 hours of repetitive high and low tide for the case IV for the different scenario of upstream river discharge (apart from experimental cases using 2D simulation) is shown in Fig. 15. The two experimental results for no upstream discharge and 5.1 l/s discharge have well represented from both the 2D and the 3D model. It can be seen that the average deposition of the sediment has been decreased with increasing upstream river flow. The increase in the upstream river flow reduces the interaction of sediment between the high tide and the tidal basin.

But in the case of reduced upstream discharge, the high tides with sediment can easily flow into the side basin then accumulate and before coming back during the low tides, major portions of the sediments can be settled down. Moreover, along with sediment interaction, the flow direction is also affected when a substantial upstream flow is provided. There is the generation of the mixed pattern of the flow direction due to the opposite forces driven by the high tides and the upstream river discharge. For the better transport and deposition of the sediment, the attached side basin should have space for high tides to come, accumulate and deposit.

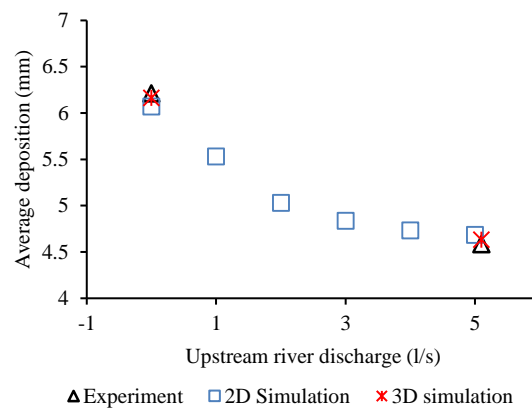


Fig. 15 Average sediment deposition for different upstream flow condition (case IV)

If there is significant upstream flow, then that space is reduced. Moreover, during the low tides also, that space is not completely emptied which ultimately reduces the effectiveness of the process. In real case also, the transported and deposited sediment during monsoon period is comparatively lower than a drier period. During monsoon period, due to the rainfall, the tidal basin is inundated to some level and the flow of the river upstream is also substantial. In such scenario, the sediment exchange could not happen from the river to the tidal basin. Furthermore, during the monsoon, the river carries a great quantity of sediment with it so it cannot erode the river bed material. Normally, the crossing dam is constructed during the drier period and low flow period. Diversion of the upstream flow is made so that around the immediate upstream of the crossing dam, artificial inundation would not happen. When the river flow starts increasing from the pre-monsoon period, the crossing dam is required to be detached.

Similarly, the average value of the sediment deposition is attempted to explore with the opening size (shown in Fig. 16). The result shows there is not a well-established relation. It shows it has a tendency to deposit more sediment with increasing opening size of the link canal. The spatial distribution of the sediment is very much important for the sustainable sediment deposition process to happen. If the deposited sediment is more pronounced on the entrance of the link canal, slowly, the rate of transport and deposition of the sediment gets reduced.

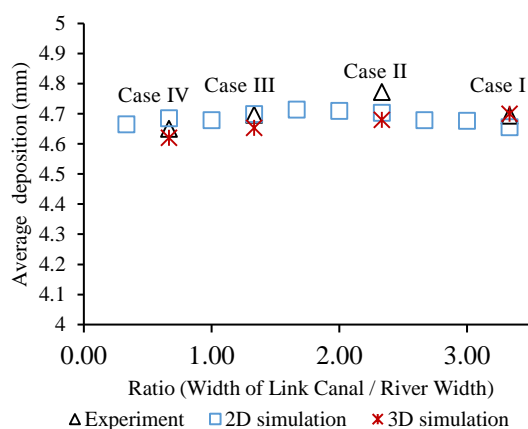


Fig. 16 Average sediment deposition for different opening sizes of the link canal

The results shown in Fig. 16 does not provide the idea about the spatial distribution. The simulation results depict the good agreement with the experimental condition except for the case II. In case II, the experimental result is a little bit higher than the simulated result. One of the reasons behind this may be during the experiment, the repetition of same hydraulic conditions of high tides and low tides may not be acquired.

The experimental domain is limited. As mentioned in the earlier chapter, due to the limited size of the attached side basin, the wall effects are clearly seen. The total or average sediment deposition on attached side basin may not completely provide reliable information in such limitation. As supported by the experimental result of the spatial distribution of the deposited sediment, the two cases with narrower opening cases (case III and case IV) showed the better effective TBM process, the numerically simulated result in those cases and other narrower opening cases are needed to examine further. The nature of the spatial distribution of the narrower opening cases (10 cm – 40 cm opening size) after 2 hours of the repetitive experimental conditions is shown in Fig. 17. With increasing the size of the opening size of the link canal, more sediment is likely to get deposited in the course of the link canal. In the case of Fig. 17 (a) and (b), the opening size is very narrow as a result of which, the flow velocity is high with high shear stress.

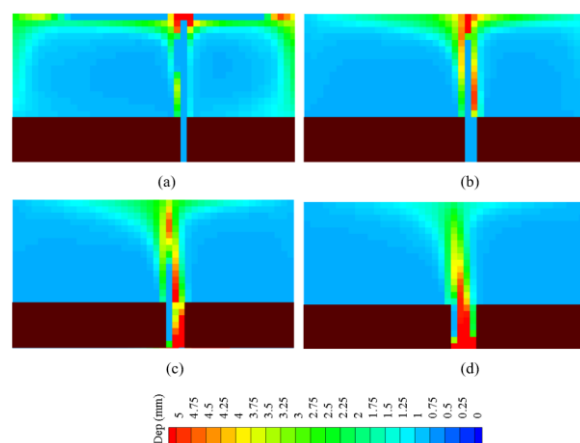


Fig. 17 Spatial distribution of the deposited sediment around the link canal for different opening sizes after 2 hour of the repetitive high and low tides (a: 10 cm, b: 20 cm, c: 30 cm and d: 40 cm)

Within the main flow direction, the deposition of the sediment doesn't happen. In the case of Fig. 17 (c) and (d), the spatial extent of the deposition is comparatively higher. If the provided case for the river is in equilibrium, the recommended size of the link canal if oriented in the proper direction is nearly equal to the river width. The Fig. 17 (c) depicts the ratio of the link canal width to the river width nearly 1.

The area near the wall of the link canal towards the tidal source has developed a complex vortex-like flow during the experiment which has a basically higher value of shear stress that erodes the sediment on that pocket. Such process is seen in all experimental cases and even in wider opening cases (shown in Photo 1). Fig. 18 shows the flow direction of the 3D simulation in the wider case (i.e. case 1). The flow directions and stream line directions show that the pocket is always hit with the higher velocity during the low tide. The water coming out from the side basin hits directly on that pocket.

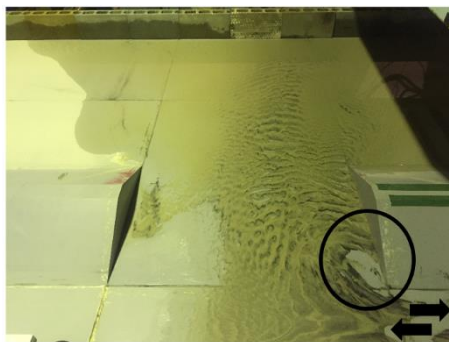


Photo 1 Typical erosion around the wall resulted by vortex like flow (case I)

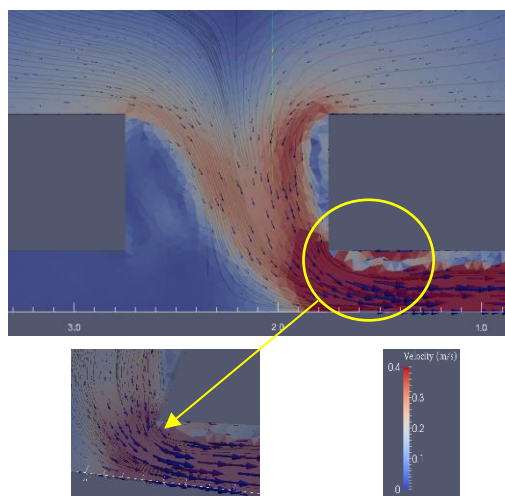


Fig. 18 Typical velocity distribution around the link canal at low tide (case I)

Even in the wider link canal area, that pocket is prone to erosion. In real case also, it happens which tried to erode the bed and bank material in that pocket. To protect from further scouring, concrete blocks are used.

## 6. Conclusions

Four cases of the experiments with different opening sizes of the link canal varying from 0.7 times the river width to thrice the river width were performed. With the supply of discharge from the downstream of the river as high tide and allowing to go back as low tide, the experiments were conducted to assess the effectiveness of TBM process. The present work discussed in the experiment is numerically simulated which shows quite good agreement for the water level, velocity, SSC and sediment deposition. The instantaneous peak fluctuation of the parameters could not be simulated but the overall value has been represented by both the 2D and the 3D numerical model. Even the developed model has not replicated the precise bed form (ripple-like structure), the overall spatial and temporal distribution of the deposited sediment has been replicated in an agreeable way. The 3D model has captured better replication than the 2D model. Since the 3D model takes a huge computation time, the 2D model has been used to explore different scenarios in experimental domain.

The limitations due to which lots of set of experimental investigations could not be done were satisfied by running the different simulations using 2D model. The developed model can be applied to simulate for the exploration of the best location of the single /multiple link canals. For the detailed physical mechanism in some local areas, the 3D model can be used to explore the spatio-temporal variation.

For the effective operation of TBM, the upstream discharge should be diverted and crossing dam should be constructed to create reduced upstream discharge condition and to allow natural tidal movement in selected tidal basin. Moreover, the opening size of the link canal more or less equal to the river width in equilibrium condition is recommended. In the real case, if the natural river is not intervened by human interactions and civil

structures, the recommended size of the link canal is more or less equal to the natural width of the river.

The experiment carried out is a preliminary stage of TBM process replication with a simple approach and it has many limitations. The research findings would be utilized in the field of sediment management. The study is focused on the land heightening of the selected tidal basin and increasing the river navigability to solve drainage congestion.

The next plan is to simulate TBM process numerically real field data of Bangladesh which is currently in progress. East *beel* Khuksia is taken as the case study area after the field visit around the SW region of Bangladesh. The fusion of utilization of natural tide movement with some level of engineering works and dredging/excavation of deposited sediment around the entrance of the link canal would strongly provide better results.

### Acknowledgements

The research is supported by JST/JICA SATREPS program on disaster prevention/mitigation measures against floods and storm surges in Bangladesh (PI: Dr. Hajime Nakagawa). The first author is pleased to acknowledge a Monbukagakusho scholarship. The authors would also express their sincere thanks to Dr. Masakazu Hashimoto for his co-operation during the development of numerical model.

### References

- Akai K, Ueda S, Sawai K (1990): Sedimentation and purification of water quality by tide in the water course with marine basins. *Techno-Ocean' 90 international symposium*. Kobe, Japan.
- Ashida K, Michiue M (1972): Studies on bed load transportation for nonuniform sediment and river bed variation. *Annals of the Disaster Prevention Research Institute, Kyoto University* **14**(B): pp. 259–273.
- Banglapedia (2012): *Banglapedia - the National Encyclopedia of Bangladesh*.
- Engelund F, Fredsøe J (1976): A Sediment Transport Model for Straight Alluvial Channels. *Nordic Hydrology* **7**: pp. 293–306.
- Haque KNH, Chowdhury FA, Khatun KR (2015): Participatory environmental governance and climate change adaptation: mainstreaming of tidal river management in south-west Bangladesh. In: Ha H (ed) *Land and Disaster Management Strategies in Asia*, pp. 189–208.
- Hashimoto M, Kawaike K, Nakagawa H, Yoneyama N (2016): Assessing the pollutant spreading using a flood simulation model in Dhaka city, Bangladesh. *IAHR APD 2016*.
- Hume TM, Herdendorf C (1993): On the use of empirical stability relationships for characterising estuaries. *J. Coastal Research* **9**: pp. 413–422.
- Ibne Amir MSI, Khan MSA, Kamal Khan MM, Golam Rasul M, Akram F (2013): Tidal river sediment management - a case study in southwestern Bangladesh. *International Journal of Civil Science and Engineering* **7**(3).
- Islam N (2001): The open approach to flood control: The way to the future in Bangladesh. *Futures* **33**(8–9): pp. 783–802. DOI: 10.1016/S0016-3287(01)00019-2.
- Iwagaki Y (1956): Fundamental study on critical tractive force. *Tans. JSCE* **41**: pp. 1–21.
- Jarrett JT (1976): *Tidal Prism - Inlet Area Relationships*. Department of Army Corps of Engineers.
- Khadim FK, Kar KK, Halder PK, Rahman MA, Morshed AKMM (2013): Integrated Water Resources Management (IWRM) Impacts in South West Coastal Zone of Bangladesh and Fact-Finding on Tidal River Management (TRM). *Journal of Water Resource and Protection* **5**(10): pp. 953–961. DOI: 10.4236/jwarp.2013.510098.
- Kibria Z (2011): *Tidal River Management (TRM) Climate Change Adaptation and Community Based River Basin Management and in Southwest Coastal Region of Bangladesh*. Uttaran: Dhaka.
- Kraus NC (1998): Inlet cross-section area calculated by process-based model. *International Conference on Coastal Engineering*. ASCE. Reston, VA, pp. 3265–3278.
- LeConte LJ (1905): Notes on the improvement of river and harbor outlets in the US. *Trans. ASCE: Discussion Paper* **55**(Dec): pp. 306–308.
- Menter FR, Ferreira JC, Esch T (2003): The SST Turbulence Model with Improved Wall Treatment for Heat Transfer Predictions in Gas Turbines. *International Gas Turbine Congress 2003* (1992):

- pp. 1–7.
- Nezu I, Nakagawa H (1993): Turbulence in open-channel flows. *IAHR Monograph*. A. A. Balkema: Rotterdam, The Netherlands.
- Nielsen P (1992): *Coastal bottom boundary layers and sediment transport. Advanced Series on Ocean Engineering*. World Scientific.
- Nowreen S, Jalal MR, Khan MSA (2014): Historical analysis of rationalizing South West coastal polders of Bangladesh. *Water Policy* **16**(2): pp. 264–279. DOI: 10.2166/wp.2013.172.
- O’Brien MP (1931): Estuary Tidal Prism Related to Entrance Areas. *Civil Engineering* **1**(8): pp. 738–739.
- O’Brien MP (1969): Equilibrium flow areas of tidal inlets on sandy coasts. *J. Waterw. Harb. Div. WW1*: pp. 43–52. DOI: 10.9753/icce.v10.25p.
- Ogawa Y, Sawai K (2013): Estuary sedimentation control using a tidal reservoir. *Advances in River Sediment Research*. CRC Press pp. 1417–1424.
- OpenCFD Ltd. (2009a): User Guide. *OpenFOAM, The Open Source CFD Toolbox*.
- OpenCFD Ltd. (2009b): Programmer’s Guide. *OpenFOAM, The Open Source CFD Toolbox*.
- Ota K, Sato T, Nakagawa H, Kawaike K (2016): Three-Dimensional Simulation of Local Scour around a Weir-Type Structure: Hybrid Euler-Lagrange Model for Bed-Material Load. *Journal of Hydraulic Engineering* **143**(4): 4016096. DOI: 10.1061/(ASCE)HY.1943-7900.0001263.
- Paul A, Nath B, Abbas MR (2013): Tidal River Management (TRM) and its implication in disaster management: A geospatial study on Hari-Teka river basin, Jessore. *International Journal of Geomatics and Geoscience* **4**(1): pp. 125–135.
- Powell MA, Thieke RJ, Mehta AJ (2006): Morphodynamic relationships for ebb and flood delta volumes at Florida’s entrances. *Ocean Dynamics* **56**: pp. 295–307.
- Rahman MZ, Islam MS, Khan ZH (2015): Tidal River Management (TRM)-An Innovative Scientific Approach for Sustainable Sediment Management. *international Conference on Recent Innovation in Civil Engineering for Sustainable Development (IICSD-2015)*, pp. 954–959.
- Rahman R, Salehin M (2013): Flood Risks and Reduction Approaches in Bangladesh. In: Shaw R, Mallick F and Islam A (eds) *Disaster Risk Reduction Approaches in Bangladesh*. Springer Japan: Tokyo, pp. 65–90.
- Rakhorst RD (2007): Delft University of Technology. Delft University of Technology.
- Rezaie AM, Naveram UK (2013): Tidal river management: An innovative approach for terminating drainage congestion and raising land through sedimentation in the Bhabodaho area, Bangladesh. *Advances in River Sediment Research*. CRC Press, pp. 1363–1375.
- Richardson JF, Zaki WN (1954): Sedimentation and fluidization; part I. *Transactions of the Institution of Chemical Engineers* **32**: pp. 35–53.
- Rubey WW (1933): Settling velocity of gravel, sand, and silt particles. *American Journal of Science*, pp. 325–338. DOI: 10.2475/ajs.s5-25.148.325.
- Shampa, Pramanik MIM (2012): Tidal River Management (TRM) for Selected Coastal Area of Bangladesh to Mitigate Drainage Congestion. *International Journal of Scientific & Technology Research* **1**(5): pp. 1–6.
- Soulsby RL, Damgaard JS (2005): Bedload sediment transport in coastal waters. *Coastal Engineering* **52**(8): pp. 673–689. DOI: 10.1016/j.coastaleng.2005.04.003.
- Staveren MF Van, Warner JF, Khan MSA (2017): Bringing in the tides. From closing down to opening up delta polders via Tidal River Management in the southwest delta of Bangladesh. *Water Policy* **19**: pp. 147–164. DOI: 10.2166/wp.2016.029.
- Stive MJF, Rakhorst RD (2008): Review of empirical relationships between inlet cross-section and tidal prism. *Journal of Water Resources and Environmental Engineering* **23**(23): pp. 89–95.
- Talchabhadel R, Nakagawa H, Kawaike K (2016a): Tidal River Management (TRM) and Tidal Basin Management (TBM): A case study on Bangladesh. *FLOODrisk 2016 - 3rd European Conference on Flood Risk Management*, pp. 1–7. DOI: 10.1051/e3sconf/20160712009.
- Talchabhadel R, Nakagawa H, Kawaike K (2016b): Experimental study on suspended sediment transport to represent Tidal Basin Management. *Journal of Japanese Society of Civil Engineers, Ser B1 (Hydraulic Engineering)* **60**: pp. 847–852.
- Talchabhadel R, Nakagawa H, Kawaike K (2016c): Experimental Study on Transportation of

- Suspended Sediment on Side Basin. *Annals of the Disaster Prevention Research Institute, Kyoto University* **59**(B): pp. 411–419.
- Talchabhadel R, Nakagawa H, Kawaike K, Hashimoto M, Sahboun N (2017a): Experimental investigation on opening size of tidal basin management: a case study in southwestern Bangladesh. *Journal of Japanese Society of Civil Engineers, Ser B1 (Hydraulic Engineering)* **61**: pp. 781–786.
- Talchabhadel R, Nakagawa H, Kawaike K, Sahboun N (2017b): Experimental study on Tidal Basin Management: A case study of Bangladesh. *E-proceedings of the 37th IAHR World Congress*.
- Tutu A (2005): River Management in Bangladesh: A People's Initiative to Solve Water-Logging. *Participatory Learning and Action* **15**(April): pp. 117–123.
- Ullah MW, Mahmud S (2017): Appropriate planning, design and implementation modalities for successful application of Tidal River Management (TRM) in coastal delta. *6th International Conference on Flood Management (ICWFM-2017)*, pp. 133–140.
- Van de Kreeke J, Haring J (1980): Stability of Estuary Mouths in the Rhine-Meuse Delta. *International Conference on Coastal Engineering, ASCE*. NY, pp. 2627–2639.
- Van Rijn LC (1984a): Sediment transport, part II: Suspended-load transport. *Journal of Hydraulic Engineering, ASCE* **110**(11): pp. 1613–1641.
- Van Rijn LC (1984b): Sediment transport - part III: Bed forms and alluvial roughness. *Journal of Hydraulic Division, ASCE* **110**(12): pp. 1733–1754.
- Wu W, Wang SSY (2006): Formulas for Sediment Porosity and Settling Velocity. *Journal of Hydraulic Engineering* **132**(8): pp. 852–862. DOI: 10.1061/(ASCE)0733-9429(2006)132:8(858)

**(Received June 13, 2017)**